Rational Design of Nonlinear Optical Materials Based on 2D Coordination Networks

Owen R. Evans and Wenbin Lin*,†

Department of Chemistry, CB#3290, University of North Carolina, Chapel Hill, North Carolina 27599

Received April 26, 2001. Revised Manuscript Received June 14, 2001

Zinc(II) and cadmium(II) coordination networks with *m*-pyridinecarboxylate bridging ligands, Zn(nicotinate)$_2$, **1**, Cd(nicotinate)$_2$, **2**, Cd{3-[2-(4-pyridyl)ethenyl]benzoate}$_2$, **3**, Zn_4-{3-[2-(4-pyridyl)ethenyl]benzoate}$_8$·{3-[2-(4-pyridyl)ethenyl]benzoic acid}·(H_2O), **4**, Zn{4-[2-(3-pyridyl)ethenyl]benzoate}$_2$·H_2O, **5**, and Zn{5-[2-(3-pyridyl)ethenyl]thiophene-2-carboxylate}$_2$, **6**, have been synthesized under hydro(solvo)thermal conditions. With the exception of **5**, these compounds adopt 2D grid structures. The use of unsymmetrical bent *m*-pyridinecarboxylate ligands leads to the formation of intrinsically acentric 2D grids which provide an interesting structural motif for the rational synthesis of polar solids. Compounds **1** and **3**−**5** are non-centrosymmetric and show significant powder second harmonic generation efficiencies. Compound **2** adopts a centrosymmetric structure due to the presence of a μ_2,η^3-carboxylate bridge, while compound **6** adopts a centrosymmetric structure due to the presence of 2-fold interpenetration. The present work illustrates the potential of rational synthesis of nonlinear-optical-active acentric solids by exploiting the propensity of the formation of 2D coordination networks based on bent linking groups. Crystal data for **1**: tetragonal space group $P4_32_12$, a = 7.709(1) Å, b = 7.709(1) Å, c = 20.327 Å, and Z = 8. Crystal data for **2**: monoclinic space group $P2_1/n$, a = 10.055(1) Å, b = 10.219(1) Å, c = 12.733(1) Å, β = 105.169(2)°, and Z = 4. Crystal data for **3**: orthorhombic space group $Fdd2$, a = 20.622(1) Å, b = 36.426(1) Å, c = 6.241(1) Å, and Z = 8. Crystal data for **4**: monoclinic space group Cc, a = 21.875(2) Å, b = 15.158(1) Å, c = 32.863(2) Å, β = 102.997(1), and Z = 4. Crystal data for **5**: orthorhombic space group $P2_12_12$, a = 7.625(1) Å, b = 25.430(2) Å, c = 5.863(1) Å, and Z = 4. Crystal data for **6**: orthorhombic space group $Pcca$, a = 17.150(2) Å, b = 9.966(1) Å, c = 12.108(2) Å, and Z = 8.

Introduction

The synthesis and characterization of solid state materials assembled from organic molecules and metal-ion building blocks continues to be an area of great interest.[1] Despite the tremendous success in the synthesis of numerous interesting metal−organic frameworks with novel topologies over the past decade,[2] few of these materials exhibit exploitable functions. Notable exceptions to the general lack of functions among coordination networks include highly porous metal carboxylates,[3] novel magnetic materials,[4] a bipyridine-based coordination network capable of catalyzing trimethylsilylcyanation of aldehydes,[5] and an enantioselective catalyst based on chiral porous metal carboxylates.[6] It has become increasingly apparent that the discovery of new coordination networks with interesting structures alone is not sufficient to sustain the rapid growth of this field. Instead more work needs to be focused on the design of metal−organic frameworks with particular functions in mind. Over the past few years, our group has become particularly interested in rational design of nonlinear optical (NLO) materials based on intrinsically acentric and chiral coordination networks.[7]

Current technologically important NLO materials are all inorganic oxides.[8] However, it is very difficult (if not impossible) to modify these materials in order to fine-tune their optical properties. On the other hand, materials chemists have extensively relied on the versa-

† E-mail: wlin@unc.edu.

(1) (a) Desiraju, G. R. *Crystal Engineering: The Design of Organic Solids*; Elsevier: New York, 1989. (b) Lehn, J.-M. *Supramolecular Chemistry: Concepts and Perspectives*; VCH Publishers: New York, 1995. (c) Quahab, L. *Chem. Mater.* **1997**, *9*, 1909−1926.

(2) (a) Zaworotko, M. J. *Chem. Soc. Rev.* **1994**, 283−288. (b) Hagrman, P. J.; Hagrman, D.; Zubieta, J. *Angew. Chem., Int. Ed.* **1999**, *38*, 2638−2684. (c) Yaghi, O. M.; Li, H.; Davis, C.; Richardson, D.; Groy, T. L. *Acc. Chem. Res.* **1998**, *31*, 474−484. (d) Munakata, M.; Wu, L. P.; Kuroda-Sowa, T. *Adv. Inorg. Chem.* **1999**, *46*, 173−304. (e) Janiak, C. *Angew. Chem., Int. Ed. Engl.* **1997**, *36*, 1431.

(3) (a) Eddaoudi, H. L.; O'Keeffe, M.; Yaghi, O. M. *Nature* **1999**, *402*, 276−279. (b) Eddaoudi, M.; Li, H.; Yaghi, O. M. *J. Am. Chem. Soc.* **2000**, *122*, 1391−1397.

(4) (a) Galan-Mascaros, J. R.; Dunbar, K. R. *Chem. Commun.* **2001**, 217−218. (b) Miller, J. S. *Inorg. Chem.* **2000**, *39*, 4392−4408.

(5) Fujita, M; Kwon, Y. J.; Washizu, S.; Ogura, K. *J. Am. Chem. Soc.* **1994**, *116*, 1151−1152.

(6) Seo, J. S.;Whang, D.; Lee, H.; Jun, S. I.; Oh, J.; Jeon, Y. J.; Kim, K. *Nature* **2000**, *404*, 982−986.

(7) (a) Evans, O. R.; Xiong, R.-G.; Wang, Z.; Wong, G. K.; Lin, W. *Angew. Chem., Int. Ed. Engl.* **1999**, *38*, 536−538. (b) Lin, W.; Ma, L.; Evans, O. R. *Chem. Commun.* **2000**, 2263−2264. (c) Evans, O. R.; Lin, W. *Chem. Mater.*, in press. (d) Lin, W.; Wang, Z.; Ma, L. *J. Am. Chem. Soc.* **1999**, *121*, 11249−11250. (e) Lin, W.; Evans, O. R.; Xiong, R.-G.; Wang, Z. *J. Am. Chem. Soc.* **1998**, *120*, 13272−13273. (f) Evans, O. R.; Wang, Z.; Lin, W. *Chem. Commun.* **1999**, 1903−1904.

(8) (a) Bossi, D. E.; Ade, R. W. *Laser Focus World* **1992**, *28* (1), 135−142. (b) Higgins, N.M. *Laser Focus World* **1992**, *28* (1), 125−133.

10.1021/cm010427k CCC: $20.00
Published on Web 08/04/2001

tility of organic synthesis to design novel organic NLO-active molecules, where their optical properties can be readily fine-tuned via systematic structural and functional group modifications.[9] Organic NLO materials have yet to find practical applications, at least in part due to the requirement of non-centrosymmetric arrangement of highly dipolar molecules in the bulk. The predominance of unfavorable centric interactions such as dipole−dipole repulsions and other non-covalent interactions has made the construction of acentric bulk materials containing highly dipolar organic NLO chromophores a challenging task.[10]

To combine the tunability of organic building blocks with the high dimensionality of oxide-based materials, we have sought to develop rational synthetic approaches to NLO-active polar solids based on metal−organic coordination networks. We envision that metal−ligand ligation can be utilized to counteract centric interactions within the bulk materials and thus greatly simplify the crystal engineering of non-centrosymmetric materials. Despite the potential importance of chiral and acentric coordination networks in second-order NLO applications, their synthesis remains essentially unexplored prior to our work,[11] presumably due to the predominant use of symmetrical linking ligands in coordination polymers.

We describe in this paper our rational approaches to the synthesis of NLO materials based on chiral and acentric infinite 2D square and rhombohedral grids, using unsymmetrical bifunctional bridging ligands *m*-pyridinecarboxylates as linking groups.[12] The basis of such a crystal engineering strategy lies on the fact that a transparent d^{10} metal center can be rendered chiral upon coordination of two pyridyl nitrogen atoms and two carboxylate moieties. The bent configuration of *m*-pyridinecarboxylates allows for a planar arrangement of metal centers to afford neutral 2D square and rhombohedral grids. The metal centers in either a *cis*-octahedral (with chelating carboxylate groups) or a tetrahedral (with monodentate carboxylate groups) environment can have at most C_{2v} symmetry and thus cannot possess a center of symmetry. Furthermore, the use of unsymmetrical bifunctional ligands ensures the absence of inversion centers on the bridging ligands. The lack of a center of symmetry on both the metal center and the bridging ligand will guarantee the acentricity of each 2D square or rhombohedral network. By utilizing *m*-pyridinecarboxylates as linking groups, we also introduce the electronic asymmetry (donor−acceptor characteristics) that is necessary for second harmonic generation. The length and conjugation of these linking groups can be increased to optimize the $\chi^{(2)}$ of these 2D square grids.[13] Therefore, it is not only possible to predict and control the solid-state structures of these 2D coordination networks, but also feasible to delineate their strucure/property relationships with the present crystal engineering strategy. This work thus demonstrates the successful rational design of NLO materials and illustrates the potential of discovering other new materials via crystal engineering of coordination networks.

Experimental Section

Materials and Methods. Unless otherwise indicated, all starting materials were purchased from Aldrich and used without further purification. *Caution*: $Zn(ClO_4)_2 \cdot 6H_2O$ and $Cd(ClO_4)_2 \cdot 6H_2O$ are potentially explosive and should be used with care! Thermogravimetric analyses (TGAs) were performed in air at a scan speed of 4 °C/min on a Shimadzu TGA-50 TG analyzer. ^1H and $^{13}C\{^1H\}$ NMR spectra were taken on a Varian Inova spectrometer at 400 and 100 MHz, respectively. Microanalyses were performed on crystalline samples by the School of Chemical Sciences Microanalytical Laboratory at the University of Illinois at Urbana−Champaign. IR spectra were recorded as KBr pellets on a Perkin-Elmer Paragon 1000 FT-IR spectrometer. All the analytical and spectroscopic data can be found in the Supporting Information.

Kurtz powder second harmonic generation measurements were performed on ground samples of crystalline **1**−**6**.[14] The powder samples have been sized to a particle size of 76 ± 13 μm. The fundamental wavelength of 1064 nm from a Nd:YAG laser was used. The powder second harmonic signals were compared to that of α-quartz to determine the relative SHG efficiencies of **1**−**6**.

Synthesis of *E*-3-[2-(4-Pyridyl)ethenyl]benzonitrile, L1. A mixture of 4-vinylpyridine (11.55 g, 110 mmol) and 3-bromobenzonitrile (18.203 g, 100 mmol) in a solution of triethylamine (25 mL) and *N*,*N*′-dimethylformamide (35 mL) was refluxed in the presence of tris(*o*-tolyl)phosphine (500 mg) and palladium(II) acetate (500 mg) for 14 h. The volatiles were removed under reduced pressure, and the resulting residue was dissolved in ethyl acetate (100 mL), washed three times with deionized water (50 mL), and dried over $MgSO_4$. Upon removing organic volatiles using a rotary evaporator, the residue was recrystallized from a solution of ethyl acetate and hexanes (1/1, (v:v)) to afford 20.0 g of pure (*E*)-3-[2-(4-pyridyl)-ethenyl]benzonitrile (97% yield).

Synthesis of *E*-4-[2-(3-Pyridyl)ethenyl]benzonitrile, L2. A mixture of (4-cyanobenzyl)triphenylphosphonium bromide (7.786 g, 17 mmol) and 3-pyridinecarbaldehyde (1.66 g, 15.5 mmol) in 30 mL of methylene chloride was stirred vigorously in a 250 mL Erlenmeyer flask. To this suspension was added 10 mL of 50% aqueous NaOH dropwise over the course of 1 h. After stirring vigorously for an additional 1 h, the mixture was washed with three portions of deionized water (100 mL). The organic layer was dried over $MgSO_4$ and evaporated to dryness. The resulting white solid was transferred to a 100 mL round-bottom flask containing iodine crystals (0.1 g, 0.788 mmol) and 40 mL of nitrobenzene, and the mixture was refluxed for 3 h. Upon cooling, the reaction mixture was extracted with dilute hydrochloric acid. The aqueous phase was removed, made alkaline with 3 M NaOH, and extracted with ethyl acetate. The extract was dried over $MgSO_4$ and evaporated to dryness to afford 2.426 g of pure product (76% yield).

Synthesis of Diethyl-3-pyridylmethyl Phosphonate. To a suspension of sodium hydride (0.361 g, 15 mmol) in anhydrous toluene (30 mL) at 0 °C was added diethyl phosphite (2.070 g, 15 mmol) dropwise over the course of 1 h. After

(9) (a) Moerner, W. E.; Silence, S. M. *Chem. Rev.* **1994**, *94*, 127−155. (b) Drost, K. J.; Jen, A. K.-Y., Rao, V. P. *ChemTech* **1995**, *25* (9), 16−25. (c) Dalton, L. R.; Harper, A. W.; Wu, B.; Ghosn, R.; Laquindanum, J.; Liang, Z.; Hubbel, A.; Xu, C. *Adv. Mater.* **1995**, *7*, 519−540. (d) Burland, D. M.; Miller, R. D.; Walsh, C. A. *Chem. Rev.* **1994**, *94*, 31−75. (e) Dalton, L. R.; Harper, A. W.; Ghosn, R.; Steier, W. H.; Ziari, M.; Fetterman, H.; Shi, Y.; Mustacich, R. V.; Jen, A. K.-Y., Shea, K. J. *Chem. Mater.* **1995**, *7*, 1060−1081.

(10) Hulliger, J.; Roth, S. W.; Quintel, A.; Bebie, H. *J. Solid State Chem.* **2000**, *152*, 49−56.

(11) Zhang, H.; Wang, X.; Teo, B.K. *J. Am. Chem. Soc.* **1996**, *118*, 11813−11821.

(12) A portion of this work has been previously communicated. See ref 2d.

(13) (a) Zyss, J. *Molecular Nonlinear Optics: Materials, Physics, and Devices*; Academic Press: New York, 1993. (b) Agulló-López, F.; Cabrera, J. M.; Agulló-Rueda, F. *Electrooptics: Phenomena, Materials and Applications*; Acdemic Press: New York, 1994.

(14) Kurtz, S. K.; Perry, T. T. *J. Appl. Phys.* **1968**, *39*, 3798−3813.

stirring for an additional 1 h at 0 °C, the mixture was refluxed for 2 h. Upon cooling, 3-chloromethylpyridine (1.27 g, 10 mmol) was added, and the mixture was refluxed for 3 h. After removing the volatiles under reduced pressure, the residue was dissolved in 50 mL of ethyl acetate, washed with two portions of deionized water, dried over $MgSO_4$, and concentrated to dryness. Silica gel chromatography eluting with a mixture of chloroform and acetone (2:1 (v:v)) afforded 0.678 g of diethyl-3-pyridylmethylphosphonate (29.6% yield).

Synthesis of *E*-5-[2-(3-Pyridyl)ethenyl]-2-bromothiophene. The yellow oil from the above was transferred to a round-bottom flask containing 5-bromo-2-thiophenecarboxaldehyde (0.515, 2.7 mmol) in 25 mL of tetrahydrofuran (THF). The mixture was chilled in a salt/ice bath, and 4 mL of a 0.97 M solution of potassium *t*-butoxide in THF was added dropwise over 1 h. The mixture was stirred for an additional 2 h and then quenched with 5 mL of deionized water. The volatiles were then removed under reduced pressure, and the residue was dissolved in ethyl acetate (50 mL), washed with three portions of deionized water (20 mL), dried over $MgSO_4$, and concentrated to dryness. Silica gel chromotagraphy eluting with a mixture of hexanes and ethyl acetate (1:1 (v/v)) afforded 0.438 g of pure *E*-5-[2-(3-pyridyl)ethenyl]-2-bromothiophene (61.0% yield).

Synthesis of 5-[2-(3-Pyridyl)ethenyl]-2-thiophenecarbonitrile, L3. The colorless oil from the above was added to a suspension of copper(I) cyanide (0.180 g, 2.0 mmol) in dimethylformamide (DMF, 25 mL) and refluxed for 12 h. After cooling, the solvent was removed under reduced pressure, and the residue was dissolved in ethyl acetate (50 mL), washed with three portions of deionized water (20 mL), dried over $MgSO_4$, and concentrated to dryness. Silica gel chromatography eluting with a mixture of hexanes and ethyl acetate afforded 0.143 g of pure *E*-5-[2-(3-pyridyl)ethenyl]-2-thiophenecarbonitrile (41.4% yield).

Synthesis of Zn(nicotinate)$_2$, 1. In a heavy-walled Pyrex tube a mixture of $Zn(ClO_4)\cdot 6H_2O$ (0.186 g, 0.5 mmol) and 3-cyanopyridine (0.105 g, 1 mmol) was thoroughly mixed in H_2O (0.2 mL) and ethanol (1 mL). The mixture was frozen in liquid nitrogen, sealed under vacuum, and placed in an oven at 130 °C. After heating for 48 h, 0.115 g of colorless rectangular crystals were obtained (yield: 74.3%). The product is air-stable and insoluble in common solvents.

Syntheis of Cd(nicotinate)$_2$, 2. In a heavy-walled Pyrex tube a mixture of $Cd(ClO_4)_2\cdot 6H_2O$ (0.055 g, 0.125 mmol) and 3-cyanopyridine (0.025 g, 0.25 mmol) was thoroughly mixed in H_2O (0.3 mL), ethanol (0.8 mL), and pyridine (0.3 mL). The mixture was frozen in liquid nitrogen, sealed under vacuum, and placed in an oven at 130 °C. After heating for 48 h, 0.036 g of colorless rectangular crystals were obtained (yield: 40.4%).

Synthesis of Cd{3-[2-(4-pyridyl)ethenyl]benzoate}$_2$, 3. In a heavy-walled Pyrex tube a mixture of $Cd(ClO_4)\cdot 6H_2O$ (0.093 g, 0.25 mmol) and **L1** (0.104 g, 0.5 mmol) was thoroughly mixed in H_2O (0.2 mL) and ethanol (1 mL). The tube was frozen in liquid nitrogen, sealed under vacuum, and placed in an oven at 130 °C. After heating for 48 h, 0.092 g of colorless needle-shaped crystals were obtained (yield: 66%).

Synthesis of Zn$_4$O{3-[2-(4-pyridyl)ethenyl]benzoato}$_8$·{3-[2-(4-pyridyl)ethenyl]benzoic acid}·H$_2$O, 4. In a heavy-walled Pyrex tube a mixture of $Zn(NO_3)_2\cdot 6H_2O$ (0.074 g, 0.25 mmol) and **L1** (0.104 g, 0.5 mmol) was thoroughly mixed in H_2O (0.3 mL), ethanol (0.7 mL), and pyridine (0.2 mL). The tube was frozen in liquid nitrogen, sealed under vacuum, and placed in an oven at 105 °C. After 72 h of heating, 0.074 g of colorless rectangular crystals were obtained (yield: 57.9% based on **L1**).

Synthesis of Zn{4-[2-(3-pyridyl)ethenyl]benzoato}$_2$·H$_2$O, 5. In a heavy-walled Pyrex tube a mixture of $Zn(ClO_4)\cdot 6H_2O$ (0.180 g, 0.5 mmol) and **L2** (0.208 g, 1.0 mmol) was thoroughly mixed in H_2O (0.05 mL) and methanol (0.5 mL). The tube was frozen in liquid nitrogen, sealed under vacuum, and placed in an oven at 130 °C. After 4 days of heating, 0.133 g of colorless rectangular crystals were obtained (yield: 50.0%).

Synthesis of Zn{5-[2-(3-pyridyl)ethenyl]thiophene-2-carboxylate}$_2$, 6. In a heavy-walled Pyrex tube a mixture of $Zn(ClO_4)\cdot 6H_2O$ (0.046 g, 0.125 mmol) and **L3** (0.053 g, 0.25 mmol) was thoroughly mixed in H_2O (0.2 mL) and ethanol (1 mL). The tube was frozen in liquid nitrogen, sealed under vacuum, and placed in an oven at 120 °C. After 4 days of heating, 0.019 g of colorless rectangular crystals were obatined (yield: 29.0%).

X-ray Structure Determinations. Data collections for compounds **1**−**6** were carried out on a Siemens SMART system equipped with a CCD detector using Mo Kα radiation with colorless crystals of dimensions of 0.05 × 0.12 × 0.40, 0.06 × 0.09 × 0.18, 0.01 × 0.10 × 0.24, 0.08 × 0.11 × 0.22, 0.08 × 0.20 × 0.42, 0.01 × 0.04 × 0.10 mm, respectively. All the structures were solved by direct methods. The structures of **1**−**3**, **5**, and **6** were refined on F^2 by full-matrix least squares using anisotropic displacement parameters for all non-hydrogen atoms.[15] Due to the large number of non-hydrogen atoms in the asymmetric unit of **4**, only Zn, O, and N atoms were refined on F^2 by full-matrix least squares using anisotropic displacement parameters, while all the carbon atoms were refined isotropically. Final refinement gave satisfactory *R* factors and goodness of fit for **1**−**6**. Experimental details for X-ray data collections of **1**−**6** are tabulated in Table 1, while selected bond distances and angles for **1**−**6** are listed in Table S1. All the drawings were made using XP[15] and CAMERON[16] programs.

Results

Synthetic Strategy. All of the metal−organic frameworks described in this article were synthesized under hydro(solvo)thermal conditions. This technique allows the formation of metastable solids not readily available from conventional methods.[17] We have previously demonstrated that under these conditions pyridinecarboxylates are readily formed from a variety of starting materials.[7,18] The in-situ slow hydrolysis of precursors containing cyano or carboxylate ester functional groups can result in phases that are not accessible from their corresponding acids. The slow hydrolysis of these precursor ligands ensures that an excess of metal ions remains in solution, thereby promoting the formation of less soluble polymeric networks. Equally important, the slow hydrolysis of these functional groups can result in the growth of large single crystals that are suitable for X-ray structure determinations and further optical studies. The coordination networks described here are all assembled utilizing zinc and cadmium metal centers. The use of d^{10} metal centers not only provides the desired coordination geometry but also ensures that these materials will be optically transparent and potentially useful for NLO applications.

Synthesis. *E*-3-(4-pyridyl)ethenylbenzonitrile, **L1**, was synthesized by a Heck coupling reaction between 4-vinylpyridine and 3-bromobenzonitrile in 93% yield. *E*-4-(3-pyridyl)ethenylbenzonitrile, **L2**, and *E*-5-[2-(3-pyridyl)ethenyl]thiophene-2-carbonitrile, **L3**, were synthesized in multisteps utilizing Wittig and Horner−Wadsworth−Emmons coupling procedures, respectively. All the intermediates and ligand precursors **L1**−**L3**

(15) *SHELX-TL*, Version 5.1; Bruker Analytical X-ray Systems, Inc.: Madison, WI, 1997.

(16) Watkin, D. J.; Prout, C. K.; Pearce, L. J. *CAMERON*; Chemical Crystallography Laboratory, University of Oxford: Oxford, U.K., 1996.

(17) (a) Laudise, R. A. *Chem. Eng. News* **1987**, *65* (39), 30−43. (b) Rabenau, A. *Angew. Chem., Int. Ed. Engl.* **1985**, *24*, 1026−1040.

(18) (a) Lin, W.; Chapman, M. E.; Wang, Z.; Yee, G. T. *Inorg. Chem.* **2000**, *39*, 4169−4173. (b) Evans, O. R.; Wang, Z.; Lin, W. *Chem. Commun.* **1999**, 1903−1904. (c) Evans, O. R.; Wang, Z.; Xiong, R.-G.; Foxman, B. M.; Lin, W. *Inorg. Chem.* **1999**, *38*, 2969−2973.

Table 1. Data for the X-ray Diffraction of 1−6[a]

	compd **1**	compd **2**	compd **3**	compd **4**	compd **5**	compd **6**
emp formula	$ZnC_{12}H_8N_2O_4$	$CdC_{12}H_8N_2O_4$	$CdC_{28}H_{20}N_2O_4$	$Zn_4C_{140}H_{103}N_9O_{19}$	$ZnC_{28}H_{22}N_2O_5$	$ZnC_{24}H_{16}N_2O_4S_2$
cryst syst	tetragonal	monoclinic	orthorhombic	monoclinic	orthorhombic	orthorhombic
a, Å	7.709(1)	10.055(1)	20.622(1)	21.875(2)	7.625(1)	17.150(2)
b, Å	7.709(1)	10.219(1)	36.426(1)	15.158(1)	25.430(2)	9.966(1)
c, Å	20.327(1)	12.733(1)	6.241(1)	32.863(2)	5.863(1)	12.108(2)
b, deg.	90	105.169(2)	90	102.997(1)	90	90
V, Å^3	1208.11(1)	1262.7(2)	4687.8(1)	10617.1(10)	1136.8(2)	2069.4(3)
Z	8	4	8	4	4	8
formula wt	309.59	356.61	560.86	2476.80	531.85	525.88
space group	$P4_32_12$	$P2_1/n$	$Fdd2$	Cc	$P2_12_12$	Pcca
T, C	75(2)	100(2)	75(2)	100(2)	75(2)	80(2)
l (Mo Ka), Å	0.710 73	0.710 73	0.710 73	0.710 73	0.710 73	0.710 73
r_{calc}, g/cm^3	1.53	1.88	1.59	1.55	1.55	1.69
m, cm^{-1} (Mo Ka)	12.8	17.4	9.7	9.8	11.3	14.3
no. of unique reflcns	1491	2006	2702	14 280	2723	1837
no. of obsd reflcns ($I > 2s(I)$)	1251	1400	2027	6295	2024	1036
N_{para}	87	172	199	765	206	182
min and max res density, e/Å^3	0.75, 2.89	0.64, 1.02	0.53, 0.75	0.48, 1.03	0.82, 0.30	0.34, 0.31
R1	0.083	0.036	0.040	0.066	0.036	0.045
wR2	0.187	0.087	0.076	0.150	0.088	0.072
goodness of fit	1.47	0.98	0.88	0.87	1.02	0.88
Flack param	0.51(5)	NA	0.01(4)	0.39(3)	0.02(2)	N/A

[a] $R1 = \sum||F_o| - |F_c|| / \sum|F_o|$; $wR2 = [\sum[w(F_o^2 - F_c^2)^2] / \sum[w(F_o^2)^2]]^{1/2}$; $GOF = [\sum[w(F_o^2 - F_c^2)^2]/(\text{no. of reflcns} - \text{no. of params})]^{1/2}$.

Scheme 1

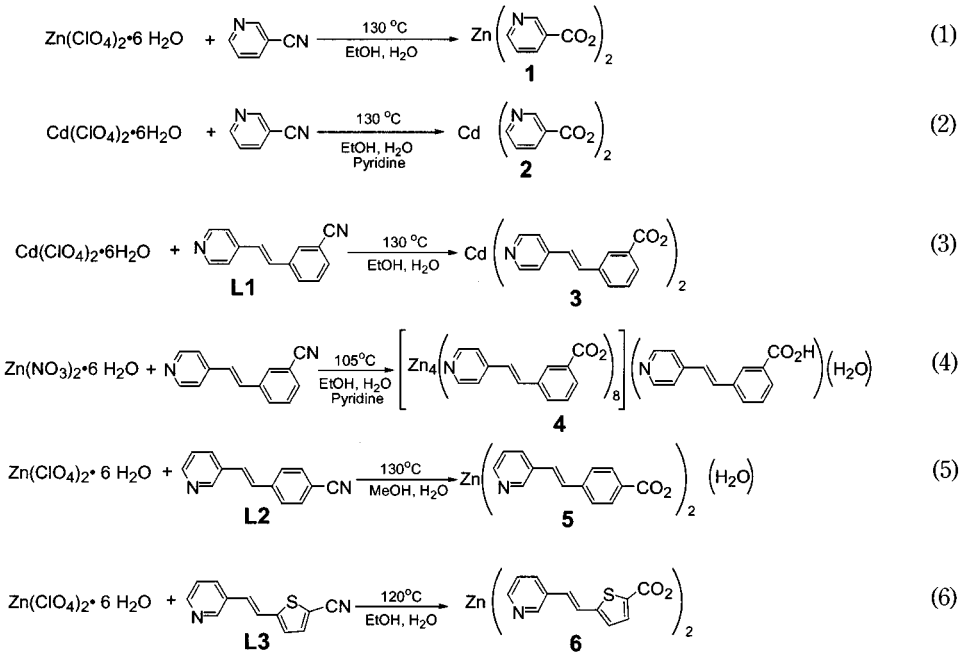

have been characterized by ^1H and $^{13}C\{^1H\}$ NMR spectroscopy.

Rectangular colorless crystals of bis(nicotinato)zinc, **1**, were obtained in 74.3% yield by a hydro(solvo)thermal reaction between $Zn(ClO_4)_2 \cdot 6H_2O$ and 3-cyanopyridine in a mixture of ethanol and water at 130 °C (eq 1 of Scheme 1). A similar reaction between $Cd(ClO_4)_2 \cdot 6H_2O$ and 3-cyanopyridine afforded Cd(nicotinate)$_2$, **2**, in 40.4% yield (eq 2 of Scheme 1). Cd{3-[2-(4-pyridyl)-ethenyl]benzoate}$_2$, **3,** was obtained in 66.0% yield via a hydro(solvo)thermal reaction between $Cd(ClO_4)_2 \cdot 6H_2O$ and (*E*)-3-(4-pyridyl)ethenylbenzonitrile, **L1**, in ethanol and water at 130 °C (eq 3 of Scheme 1). A similar reaction between $Zn(NO_3)_2 \cdot 6H_2O$ and **L1** in a mixture of ethanol, water, and pyridine at 105 °C afforded Zn_4-{3-[2-(4-pyridyl)ethenyl]benzoato}$_8$·{3-[2-(4-pyridyl)ethenyl]benzoic acid}·H_2O, **4**, in 57.9% yield (eq 4 of Scheme 1). Compound **5**, Zn{4-[2-(3-pyridyl)ethenyl]benzoate}$_2$·H_2O, was obtained in 50.0% yield via a hydro(solvo)-thermal reaction between (*E*)-4-(3-pyridyl)ethenylbenzonitrile, **L2**, and $Zn(ClO_4)_2 \cdot 6H_2O$ in methanol and water at 130 °C (eq 5 of Scheme 1). Compound **6**, Zn-{5-[2-(3-pyridyl)ethenyl]thiophene-2-carboxylate}$_2$, was prepared by a hydro(solvo)thermal reaction between Zn-$(ClO_4)_2 \cdot 6H_2O$ and 5-[2-(3-pyridyl)ethenyl]thiophene-2-carbonitrile in a mixture of ethanol and water in 29% yield (eq 6 of Scheme 1). The IR spectra of **1**−**6** clearly show the presence of carboxylate groups and the absence of peaks indicative of perchlorate anions or cyano groups. In addition, the symmetric C═O stretches for **1**, **3**, and **4** occur at ∼1400 cm^{-1}, while the symmetric C═O stretches for **5** and **6** appear at 1345 and 1353 cm^{-1}, respectively.[19] The position of these stretches

(19) Mehrotra, R. C.; Bohra, R. *Metal Carboxylates*; Academic Press: New York, 1983.

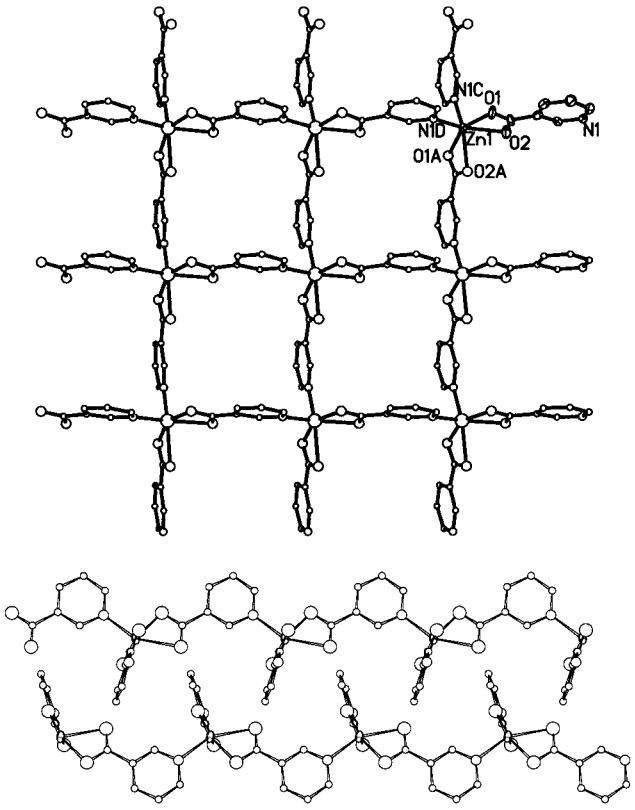

Figure 1. (a, top) View of 2D square grid structure of **1**. The asymmetric unit is shown in ellipsoids at 50% probability. The circles with increasing sizes represent C, N, O, and Zn atoms, respectively. (b, bottom) Interdigitation of adjacent square grids in **1** as viewed down the *b* axis. The $\pi-\pi$ stacks formed between the pyridyl rings are clearly visible.

suggest that **1**, **3**, and **4** possess chelating carboxylate groups, while **5** and **6** contain monodentate carboxylate groups. The symmetric stretch of **2** appears as a very broad peak at 1406 cm^{-1}, suggesting the presence of triply bridging carboxylate.

X-ray Structure of Zn(nicotinate)$_2$, 1. A single-crystal X-ray diffraction study of **1** revealed an infinite 2D square grid structure consisting of six-coordinate Zn centers and bridging nicotinate groups (Zn−Zn separation of 7.71(1) Å). A portion of the 2D grid is shown in Figure 1a, where half of a zinc atom and one exo-tridentate nicotinate group are crystallographically unique. Compound **1** crystallizes in chiral space group $P4_32_12$. The zinc center lies on a crystallographic 2-fold axis and is coordinated in a cis-configuration to two carboxylate groups and to two pyridyl nitrogen atoms of four different nicotinate groups. The carboxylate groups bind to the zinc center in a semi-chelating fashion with a Zn−O1 distance of 2.008(5) Å and a Zn−O2 distance of 2.385(5) Å. The overall geometry around the zinc center is a highly distorted octahedron with the cis-bond angles ranging from 58.8(2) to 104.0(2)°. The zinc centers in **1** possess C_2 symmetry. As a result, all the zinc centers are chiral and have the same handedness (δ). Compound **1** represents a rare example of a chiral 2D infinite square grid.

The zinc atoms in a single grid of **1** all lie on the same plane. However, the disposition of the bridging nicotinate group allows the interdigitation of adjacent layers and the formation of aromatic $\pi-\pi$ stacks along the *c* axis (Figure 1b). This $\pi-\pi$ stacking, an interaction well-known in supramolecular chemistry,[1] not only leads to increased thermodynamic stability but also effectively fills the void space of the square grid. As a result, no solvent molecules are enclathrated in **1**. Moreover, the $\pi-\pi$ stacking interactions between the pyridyl rings of the nicotinate groups have ensured the packing of chiral square grids in **1** into a bulk chiral solid.

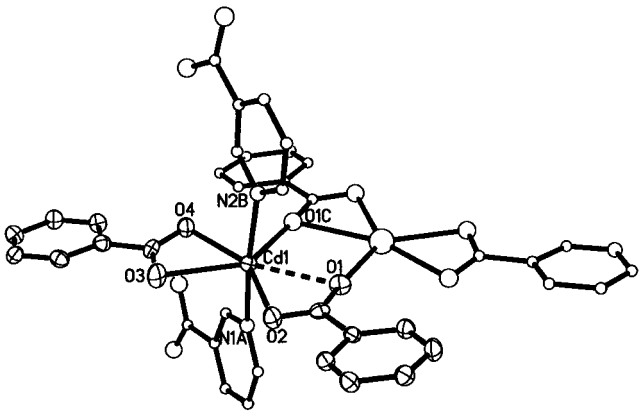

Figure 2. Coordination environment of **2**. The asymmetric unit is shown in ellipsoids at 50% probability, while the circles with increasing sizes represent C, N, O, and Cd atoms, respectively.

X-ray Structure of Cd(nicotinate)$_2$, 2. Compound **2** crystallizes in monoclinic space group $P2_1/n$. The asymmetric unit contains one cadmium center and two nicotinate ligands. All atoms lie on general positions. Each cadmium center in **2** coordinates to five carboxylate oxygens and two pyridyl nitrogen atoms of five different nicotinate ligands (Figure 2). The O3−C7−O4 carboxylate coordinates in a chelating fashion with a Cd1−O4 distance of 2.315(4) Å and a Cd1−O3 distance of 2.522(4) Å, while the O1−C1−O2 carboxylate coordinates in a semi-chelating fashion with a Cd1−O2 distance of 2.270(4) Å and a Cd1−O1 distance of 2.640-(4) Å. The O1 center also coordinates to a second Cd center to bridge adjacent Cd centers to form a dimetal linkage, and thus the nicotinate group adopts an *exo*-tetradentate bridging mode. The *exo*-tetradentate nicotinate ligands serve to link adjacent dimetal units to form 2D network running along the diagonal of the *ac* plane (Figure S1), while the *exo*-tridentate nicotinate groups link Cd centers to form a 2_1 helix along the *b* axis (Figure S2). The 2D network formed by the Cd centers, and the *exo*-tetradentate nicotinate ligands are thus cross-linked by the *exo*-tridentate nicotinate groups to form a complex 3D structure (Figure 3). Compound 2 adopts a centrosymmetric structure as a consequence of the μ_2,η^3-carboxylate bridge.

X-ray Structure of Cd{3-[2-(4-pyridyl)ethenyl]-benzoate}$_2$, 3. Compound **3** crystallizes in orthorhombic space group *Fdd*2. The asymmetric unit in **3** consists of one Cd center and one bridging 3-[2-(4-pyridyl)-ethenyl]benzoate group (Figure 4a). The cadmium center lies on a 2-fold crystallographic axis and coordinates to two carboxylate groups and to two pyridyl nitrogen atoms of four different 3-[2-(4-pyrdyl)ethenyl]benzoate groups in a *cis*-octahedral fashion. Each of the cadmium atoms in **3** adopts a highly distorted octahedron, with the carboxylate groups coordinating to the metal center in chelating fashion with a Cd−O4 distance of 2.273(6) Å and a Cd−O2 distance of 2.484(4) Å.

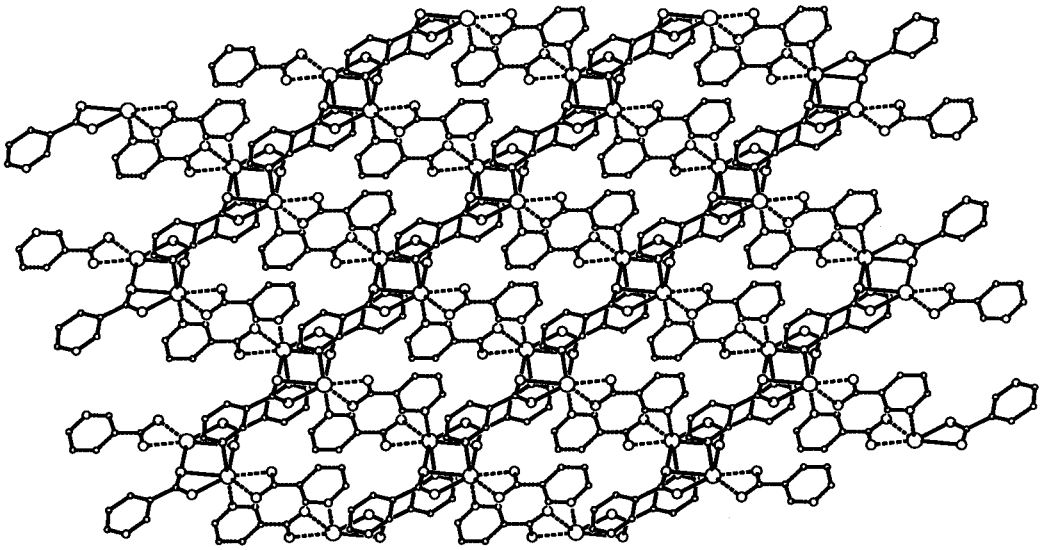

Figure 3. View of 3D network structure of **2** down the *c* axis. The solid and dashed lines correspond to the 2D network and 2_1 helix shown in Figure 4a,b, respectively.

The bent geometry of the bridging *m*-pyridinecarboxylate ligands has allowed the formation of an infinite 2D grid structure (Figure 4a). The rhombohedral grid in **3** has Cd−Cd separations of 13.92(6) Å, and Cd−Cd−Cd angles of 84.5 and 95.5°, respectively. At first glance, **3** appears to have a large void space within the rhombohedral grid. The void space is in fact effectively filled via the parallel interweaving of three independent rhombohedral grids (Figure 4b). The cadmium centers in **3** have C_2 symmetry and are thus chiral. Each rhombohedral grid in **3** is chiral. Unlike **1,** however, a glide plane relates adjacent layers of 3-fold interwoven rhombohedral grids, resulting in an inversion of chirality between metal centers of adjacent layers. As a result, adjacent layers have opposite chirality, and **3** is a supramolecular racemate. Fortunately, there exist no inversion centers among adjacent layers, and **3** is a noncentrosymmetric solid. The control of the packing in the third dimension thus presents a challenge in the crystal engineering of acentric and chiral solids based on 2D networks.

X-ray Structure of Zn_4\{3-[2-(4-pyridyl)ethenyl]-benzoato\}$_8$·\{3-[2-(4-pyridyl)ethenyl]benzoic acid\}·H_2O, 4. Compound **4** crystallizes in acentric space group *Cc*. The asymmetric unit contains four zinc centers, eight 3-[2-(4-pyridyl)ethenyl]benzoate ligands, one guest water, and one 3-[2-(4-pyridyl)ethenyl]benzoic acid. Each of the zinc centers in **4** coordinates to two pyridyl nitrogen atoms and to two carboxylate groups from four different 3-[2-(4-pyridyl)ethenyl]benzoate ligands in a distorted *cis*-octahedral fashion (Figure 5a).

Each zinc center in **4** is connected to four adjacent crystallographically equivalent zinc centers through 3-[2-(4-pyridyl)ethenyl]benzoate bridges to result in an infinite rhombohedral grid. The Zn−Zn separations in these grids are 13.30 Å, while the Zn−Zn−Zn angles are 69.4 and 110.6°. Because the asymmetric unit contains four zinc centers, they are bridged by the *m*-pyridinecarboxylate ligands to afford four independent 2D grids that lie in the *ab* plane. While the four independent grids are topologically identical, their stacking along the *c*-axis is considerably more complex. The grids stack in a repeating ABC sequence (Figure 5b). The two rhombohedral grids formed from the Zn1 and Zn4 centers exhibit 2-fold interweaving (A sequence), while those formed from the Zn2 and Zn3 centers interdigitate through the aromatic $\pi-\pi$ stacks (B and C sequences, respectively). The void space left after such interdigitation is filled with free 3-[2-(4-pyridyl)ethenyl]benzoic acid molecules. It is remarkable that there exist aromatic $\pi-\pi$ stacking, interweaving, and inclusion of guest molecules in **4**, yet a noncentrosymmetric bulk solid is obtained.

Structure of Zn\{4-[2-(3-pyridyl)ethenyl]benzoate\}$_2$·H_2O, 5. Compound **5** crystallizes in the chiral space group $P2_12_12$. The asymmetric unit contains one zinc atom lying on a crystallographic 2-fold axis and one bridging 4-[2-(3-pyridyl)ethenyl]benzoate group. The zinc center coordinates to two carboxylate groups in a monodentate fashion and to two pyridyl nitrogen atoms of four different 4-[2-(3-pyridyl)ethenyl]benzoate groups to result in an infinite 2D rhombohedral grid with a Zn−Zn separation of 13.58 Å (Figure 6a). Each zinc center in **5** has C_2 molecular symmetry and is thus inherently chiral. It is evident from Figure 6a that all the Zn centers in each 2D rhombohedral grid have the same chirality. The rhombohedron is highly distorted and elongated along the *a* axis with the Zn−Zn−Zn angles of 32.6 and 138.9°. As a consequence of this distortion, the rhombohedral grid has minimal void space to accommodate one included water molecule, and no interweaving is observed.

Examinations of **5** along the *a* and *b* axes indicate that adjacent rows of Zn centers in each 2D grid are offset by 2.93 Å along the *c* axis, and therefore all the 2D grids are pleated (Figure 6b). The puckered nature of the 2D grids renders perfect interlayer registry and provides an interesting mechanism for controlling the stacking of all the 2D grids along the *c* axis and facilitating the crystal engineering of chiral 2D coordination polymers.

Structure of Zn\{5-[2-(3-pyridyl)ethenyl]thiophene-2-carboxylate\}$_2$, 6. Compound **6** crystallizes in the centrosymmetric space group *Pcca*. The zinc center lies on a crystallographic 2-fold axis, with one zinc center and one 5-[2-(3-pyridyl)ethenyl]thiophene-2-carboxylate bridging group in the asymmetric unit. The

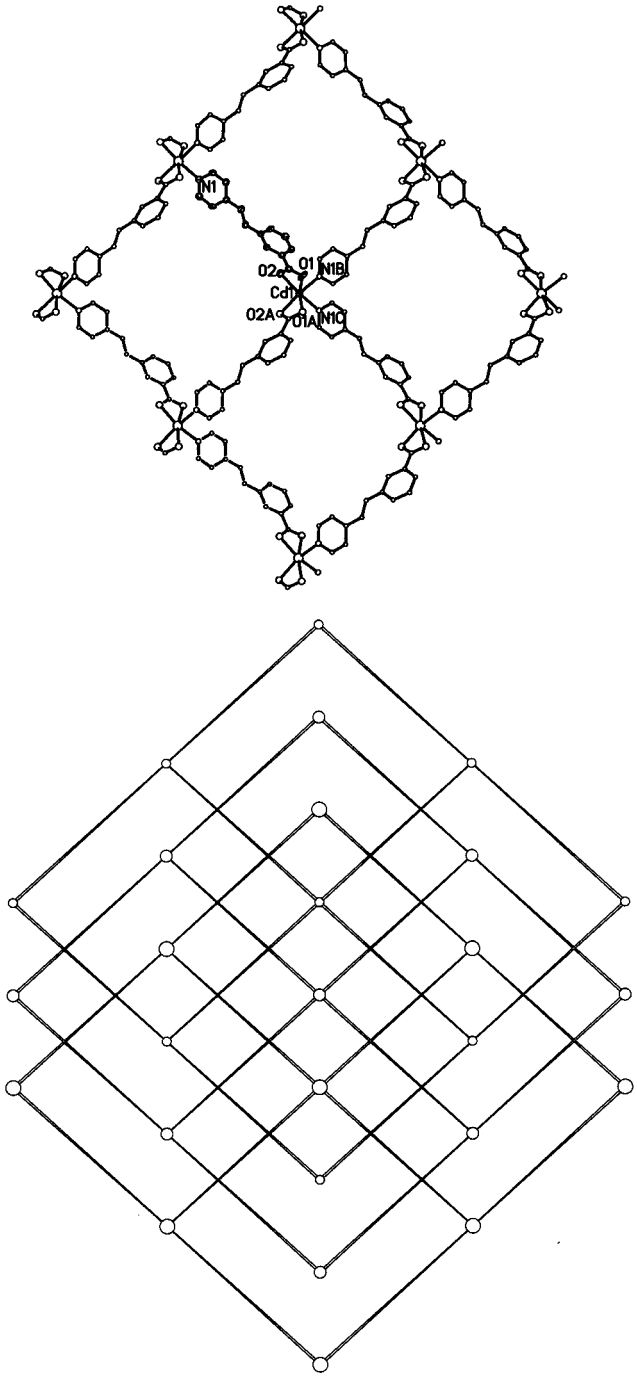

Figure 4. (a, top) View of 2D rhombohedral grid structure of **3**. The asymmetric unit is shown in ellipsoids at 50% probability, while the circles with increasing sizes represent C, N, O, and Cd atoms, respectively. (b, bottom) A schematic showing the interweaving of three independent rhombohedral grids in the *ac* plane in **3**.

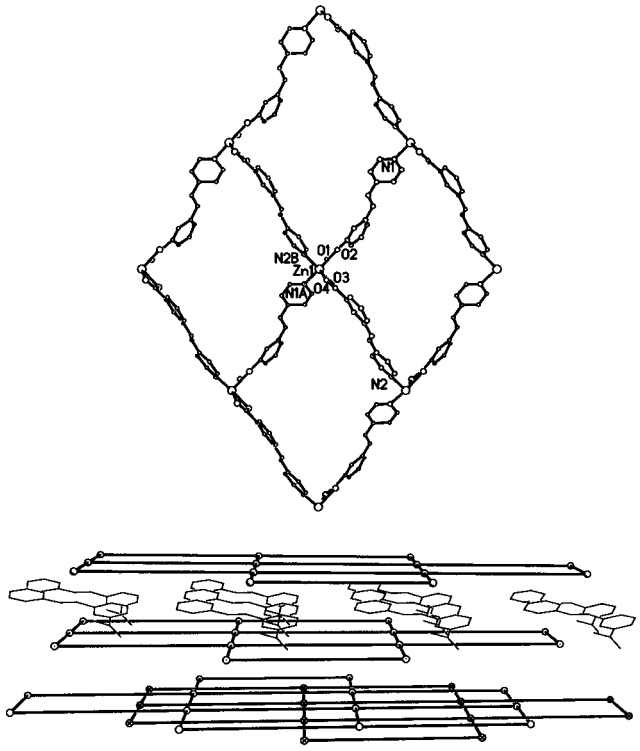

Figure 5. (a, top) View of 2D rhombohedral grid structure formed by Zn1 centers in **4**. (b, bottom) Stacking of four independent 2D rhombohedral grids along the *c* axis. From bottom to top, interweaving of the grids formed by Zn1 and Zn4 centers, the grid formed by the Zn3 centers, and the grid formed by the Zn2 Centers stack in ABC sequence. Free 3-[2-(4-pyridyl)ethenyl]benzoic acid is sandwiched between the grids formed by Zn3 and Zn2 centers.

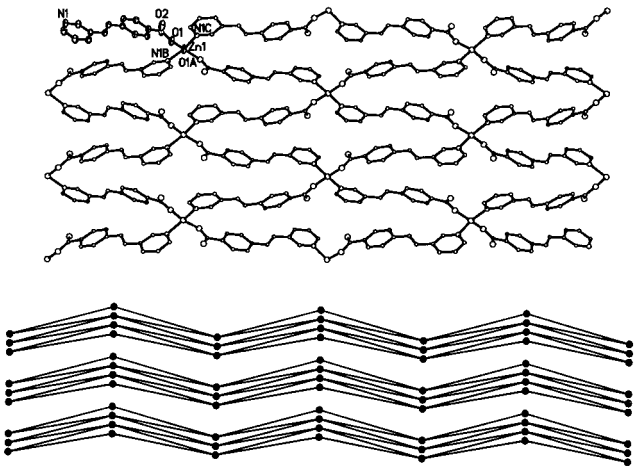

Figure 6. (a, top) View of the 2D rhombohedral grid of **5**. The ellipsoids represent the asymmetric unit. The circles with increasing sizes represent C, N, O, and Zn, respectively. (b, bottom) Stacking of adjacent 2D pleated sheets in **5** as shown approximately down the crystallographic direction [110]. Only the zinc atoms are shown.

local coordination geometry about the zinc center can best be described as a distorted tetrahedron. The O2−Zn1−O2 carboxylate group coordinates in a monodentate fashion with a Zn1−O2 distance of 1.988(8) Å and a Zn1−O1 distance of 2.758(9) Å. The bond angles about the Zn1 tetrahedron range from 95.2 to 124.9° and deviate slightly from those of a perfect tetrahedron. The Zn1 center coordinates to two pyridyl nitrogen atoms and to two carboxylate oxygen atoms of four different 3-[2-(3-pyridyl)ethenyl]thiophenecarboxylate ligands to result in an infinite 2D rhombohedral grid with a Zn−Zn separation of 13.33 Å (Figure 7a). In contrast to **5**, the rhombohedral grid in **6** is less distorted with Zn−Zn−Zn angles of 80.05 and 96.74°. There is thus more void space inside each rhombohedral grid in **6** to result in a 2-fold interweaved structure (Figure 7b). The two interweaved rhombohedral grids are structurally identical and are related to each other through an inversion center. Although the adjacent rows of Zn centers in each

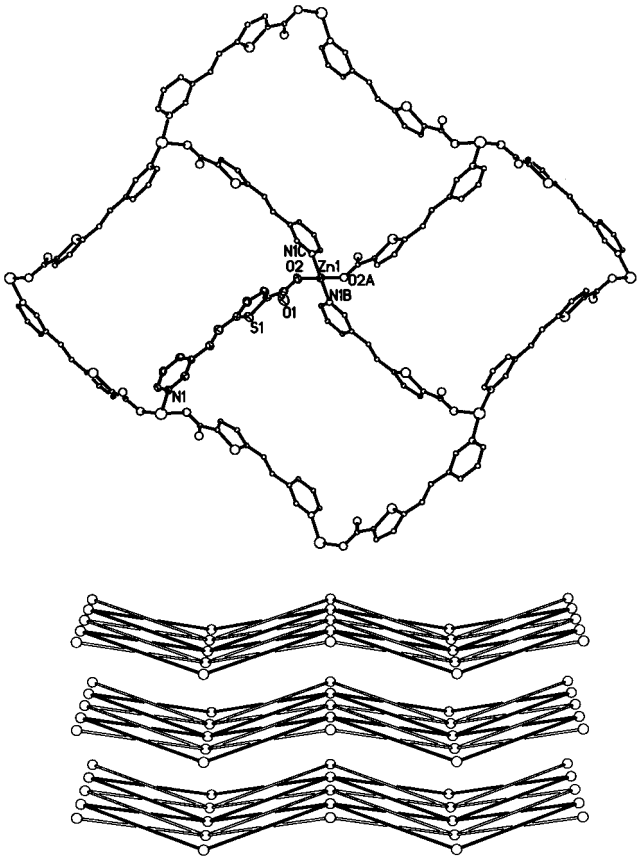

Figure 7. (a, top) View of the 2D rhombohedral grid of **6**. The ellipsoids represent the asymmetric unit. The circles with increasing sizes represent C, N, O, and Zn, respectively. (b, bottom) Schematic showing stacking of ruffled 2-fold interweaved 2D rhombohedral grids of **6.** Only the zinc atoms are shown.

2D grid of **6** are also offset along the *c* axis to result in pleated sheet topology as seen in **5** (Figure 7b), compound **6** is centrosymmteric because of the 2-fold interweaving.

Powder Second Harmonic Generation Results. We have performed Kurtz powder second harmonic generation studies using the 1064 nm fundamental wavelength of a Nd:YAG laser. Consistent with their non-centrosymmetric structures, compounds **1**, **3**, **4**, and **5** are SHG-active. Compound **1** exhibits a modest powder SHG efficiency ($I^{2\omega}$ of 2 vs α-quartz). The low value of $I^{2\omega}$ is due in part to the short ligand length (and thus inefficient conjugation) in **1**. In contrast, compound **3** has a much larger SHG response ($I^{2\omega}$ of 800 vs α-quartz). In comparison to technologically important $LiNbO_3$, which has a powder SHG intensity of 600 vs α-quartz,[14] the SHG response of **3** is remarkable. Compound **4** also exhibits a substantial SHG response with an $I^{2\omega}$ of 400 vs α-quartz. Compound **5** exhibited a large SHG response, but the sample was damaged by the laser before an accurate measurement could be attained (attempts to attenuate the input beam were unsuccessful). Compounds **2** and **6** exhibit no SHG response, consistent with their centrosymmetric structures.

Compounds **1**−**6** are thermally robust and are insoluble in common solvents (Figure 8). Furthermore, the use of d^{10} metal centers ensures that **1**−**6** are optically transparent. Because only modest donor/acceptor combinations were used in these compounds, we have also overcome severe optical absorption problems often encountered in purely organic NLO materials. These results clearly demonstrate that efficient NLO materials can be synthesized based on coordination networks with 2D grid structures.

Discussion. With the exception of **5**, the use of *m*-pyridinecarboxylates as bridging ligands has resulted in the formation of 2D square or rhombohedral grids. The use of symmetrical bridging ligands such as bipyridine or terephalate in the synthesis of infinite 2D grids has now become commonplace. The use of such ligands often leads to centrosymmetric structures due to their symmetrical nature. The use of unsymmetrical bridging ligands such as *m*-pyridinecarboxylates is key to the

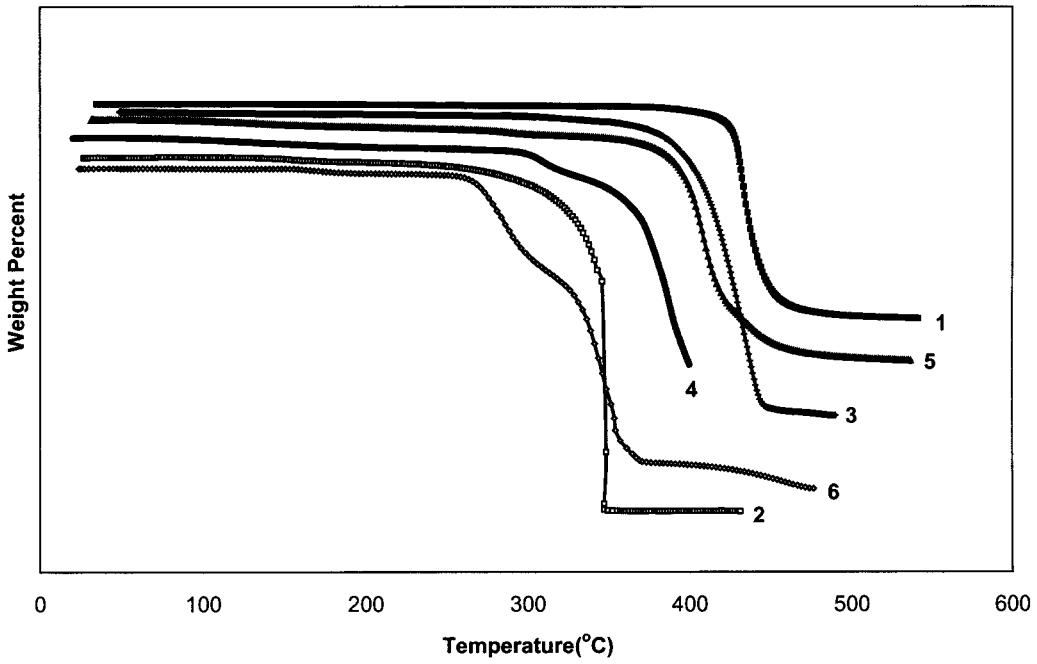

Figure 8. TGA curves for compounds **1**−**6**. For clarity, the curves have been shifted vertically.

construction of acentric solids based on 2D grids. Each metal center in these networks has at most C_2 molecular symmetry and therefore guarantees that each individual grid is acentric. The synthesis of coordination polymers based on unsymmetrical bridging ligands is inherently more difficult owing to the varied coordination ability of different functional groups. We have overcome such a difficulty by employing a combination of hydro(solvo)-thermal conditions and well-chosen ligand precursors. The in-situ slow hydrolysis of these precursor ligands under such conditions ensures that an excess of metal ions remains in solution, thereby favoring the formation of less soluble polymeric networks. Our work thus clearly shows that acentric square and rhombohedral grids can be readily designed using this very simple approach. However, several other factors need to be controlled in order to rationally design acentric solids based on 2D grids.

While **1** adopts a chiral 2D grid structure, **2** crystallizes in a centrosymmetric 3D structure. This result suggests that the formation of 2D grids is affected by the changes in atomic radii and coordination environments of the metal connecting points. This trend is also observed in the structures of **3**−**6**. Although both **3** and **4** adopt 2D grid structures, they have very different network topologies. Despite numerous attempts, we have not even been able to isolate neutral Cd(II) phases based on 4-[2-(3-pyridyl)ethenyl]benzoate and 3-[2-(3-pyridyl)ethenyl]thiophenecarboxylate ligands. Such a drastic difference as a result of the metal connecting points is in stark contrast to the crystal engineering of acentric solids based on 3D diamondoid networks. In our earlier work, we have shown that the formation of 3D diamondoid networks is not sensitive to the differences in atomic radii and coordination environments of the metal connecting points.[7a−c] In almost all the cases, both Zn- and Cd-based 3D diamondoid networks adopt the same topologies despite their differences in atomic radii and coordination environments. The different degree of control on the packing along the third dimension is presumably responsible for different behaviors between the 2D grid and 3D diamondoid networks.

Numerous interpenetrated infinite networks have been reported in the literature. We have previously documented this phenomenon in the synthesis of 3D diamondoid coordination polymers.[7a−c] To enhance the SHG properties of metal−organic coordination networks, ligands with increasing length (and hence conjugation) are desired. Unfortunately, such increase in ligand length results in larger cavities formed within each 2D grid, which often leads to interpenetration (or interweaving) of independent 2D grids (in order to effectively fill the void space). For example, compound **1** effectively fills the void space within each 2D grid via interdigitation of the other 2D grid, whereas **3** and **4** adopts 3- and 2-fold interweaving, respectively, in order to fill the void space. The interpenetration (or interweaving) of independent nets complicates the crystal engineering of acentric solids; an even-fold interpenetration can (but not necessarily) bring inversion symmetry and cause the resulting structure to be centrosymmetric. For example, compound **6** adopts 2-fold interweaving and crystallizes in a centrosymmetric space group. Just as in 3D diamondoid coordination networks, the number of interpenetrated nets is directly correlated to the ligand length. With judicious choices of bridging ligands of desired lengths, an odd-number-fold of interpenetration (interweaving) can be achieved and acentric 2D grids can be designed.

Finally, it is also necessary to control the stacking of non-centrosymmetric 2D grids in the third dimension in order to obtain a bulk acentric solid. Inherent in the design of these infinite planar 2D grids is the lack of control in the third dimension. For example, the metal centers in adjacent layers in compound **3** have opposite chirality to result in a 2D racemate. While the grids in **3** are related via a glide plane, this lack of control could bring unwanted inversion centers. To ensure bulk acentricity, we have utilized *m*-pyridinecarboxylates ligands in which the pyridyl nitrogen is situated in a meta-position to design 2D square grids that exhibit a corrugated (or pleated) topology as in **5** and **6**. The ruffled nature of these networks possesses better interlayer registry and thus promotes the stacking of 2D grids in a fashion that adjacent layers are related only by translational symmetry. Bulk chirality is maintained in compound **5** via such in-registry stacking of adjacent 2D grids. However, 2-fold interweaving has caused **6** to adopt a centrosymmetric structure. Acentric solids can thus be rationally synthesized by controlling the degree of interweaving of 2D grids with a pleated topology. We have therefore demonstrated a successful crystal engineering approach toward the synthesis of NLO materials based on infinite 2D grids.

Acknowledgment. We acknowledge NSF (Grant CHE-9875544) for financial support. We also thank Dr. Scott R. Wilson and the Materials Chemistry Laboratory at University of Illinois at Urbana−Champaign for X-ray data collections. We thank Dr. R. Xiong and Dr. Z. Wang for help with initial experiments and Dr. I. Y. Chan for access to his laser setup. W.L. is an Alfred P. Sloan Fellow, an Arnold and Mabel Beckman Young Investigator, and a Cottrell Scholar of Research Corp.

Supporting Information Available: Spectroscopic and analytical data, one table, and two figures (PDF) and crystallographic information (CIF). This material is available free of charge via the Internet at http://pubs. acs.org

CM010427K